

# The Cth2 ARE-binding Protein Recruits the Dhh1 Helicase to Promote the Decay of Succinate Dehydrogenase *SDH4* mRNA in Response to Iron Deficiency<sup>\*[5]</sup>

Received for publication, June 27, 2008, and in revised form, July 31, 2008. Published, JBC Papers in Press, August 20, 2008, DOI 10.1074/jbc.M804910200

Elisa Pedro-Segura<sup>†1</sup>, Sandra V. Vergara<sup>§2</sup>, Susana Rodríguez-Navarro<sup>¶3</sup>, Roy Parker<sup>||</sup>, Dennis J. Thiele<sup>§</sup>, and Sergi Puig<sup>‡4</sup>

From the <sup>†</sup>Departament de Bioquímica i Biologia Molecular, Universitat de València, Avenida Doctor Moliner 50, E-46100, Burjassot, València, Spain, the <sup>§</sup>Department of Pharmacology and Cancer Biology, Duke University, Medical Center, Research Drive, Durham, North Carolina 27710, the <sup>¶</sup>Centro de Investigación Príncipe Felipe, Autopista del Saler 16, E-46013, València, Spain, and the <sup>||</sup>Department of Molecular and Cellular Biology, and Howard Hughes Medical Institute, University of Arizona, Tucson, Arizona 85721

Iron is an essential nutrient that participates as a redox co-factor in a broad range of cellular processes. In response to iron deficiency, the budding yeast *Saccharomyces cerevisiae* induces the expression of the Cth1 and Cth2 mRNA-binding proteins to promote a genome-wide remodeling of cellular metabolism that contributes to the optimal utilization of iron. Cth1 and Cth2 proteins bind to specific AU-rich elements within the 3'-untranslated region of many mRNAs encoding proteins involved in iron-dependent pathways, thereby promoting their degradation. Here, we show that the DEAD box Dhh1 helicase plays a crucial role in the mechanism of Cth2-mediated mRNA turnover. Yeast two-hybrid experiments indicate that Cth2 protein interacts *in vivo* with the carboxyl-terminal domain of Dhh1. We demonstrate that the degradation of succinate dehydrogenase *SDH4* mRNA, a known target of Cth2 on iron-deficient conditions, depends on Dhh1. In addition, we localize the Cth2 protein to cytoplasmic processing bodies in strains defective in the 5' to 3' mRNA decay pathway. Finally, the degradation of trapped *SDH4* mRNA intermediates by Cth2 supports the 5' to 3' directionality of mRNA turnover. Taken together, these results suggest that Cth2 protein recruits the Dhh1 helicase to ARE-containing mRNAs to promote mRNA decay.

All eukaryotes require iron as an essential micronutrient because of its ability to participate as a redox co-factor in a wide

range of cellular processes including oxygen transport, mitochondrial oxidative phosphorylation, lipid metabolism, DNA replication and repair, and microbial infections. Although iron is abundant, its bioavailability is highly restricted under aerobic conditions because of the insolubility of ferric hydroxides at physiological pH. In fact, iron deficiency anemia represents the primary nutritional disorder in the world, estimated to affect over two billion people (1). Living organisms have developed sophisticated transcriptional and post-transcriptional mechanisms to optimize iron acquisition and utilization during scarcity (2–6).

The budding yeast *Saccharomyces cerevisiae* utilizes two complementary strategies in response to the depletion of iron. First, the Aft1 and Aft2 iron-sensing transcription factors induce the expression of a set of genes involved in the acquisition of extracellular iron and its mobilization from intracellular iron stores (7–9). Second, a global metabolic remodeling prioritizes the utilization of the limited iron within the cell. Optimization of cellular iron utilization is coordinated by two additional Aft1/Aft2 targets: the RNA-binding proteins Cth1 and Cth2 (10, 11). Cth1 and Cth2 proteins contain tandem CX<sub>8</sub>CX<sub>5</sub>CX<sub>3</sub>H-type zinc finger motifs responsible for binding to AU-rich elements (ARE)<sup>5</sup> located within the 3'-untranslated region (UTR) of target mRNAs, such as the succinate dehydrogenase subunit encoded by the *SDH4* gene (10, 11). In response to iron deficiency, Cth1 and Cth2 promote the degradation of many ARE-containing mRNAs encoding iron-binding proteins or enzymes that participate in metabolic pathways that use iron as a co-factor such as the tricarboxylic acid cycle, mitochondrial respiration, heme biosynthesis, and fatty acid synthesis (10).

Biochemical and genetic studies on mRNA decay in yeast and mammalian cells have identified two general pathways for mRNA turnover in eukaryotic cells (reviewed in Refs. 12 and 13). Both pathways initiate with the shortening of the poly(A) tail by the major cytoplasmic Ccr4/Pop2/Not deadenylase complex. Deadenylation can be followed by 3' to 5' mRNA

<sup>\*</sup> This work was supported, in whole or in part, by National Institutes of Health Grant GM041840 (to D. J. T.) and National Institutes of Health Predoctoral Fellowship FDK081304A (to S. V. V.). This work was also supported by Spanish Ministerio de Educación y Ciencia Grant BIO2005-07120, Generalitat Valenciana Grant GV05-081, and FEDER funds from the European Community (to S. P.). The costs of publication of this article were defrayed in part by the payment of page charges. This article must therefore be hereby marked "advertisement" in accordance with 18 U.S.C. Section 1734 solely to indicate this fact.

<sup>[5]</sup> The on-line version of this article (available at <http://www.jbc.org>) contains supplemental Tables S1 and S2 and Figs. S1–S4.

<sup>1</sup> Recipient of a predoctoral V Segles fellowship from the University of Valencia.

<sup>2</sup> Trainee of the Duke University Program in Genetics and Genomics.

<sup>3</sup> Recipient of a Ramón y Cajal contract with the Centro de Investigación Príncipe Felipe.

<sup>4</sup> Recipient of a Ramón y Cajal contract with the Universitat de València. Recipient of an EMBO short term fellowship. To whom correspondence should be addressed: Tel.: 34-963543021; Fax: 34-963544635; E-mail: sergi.puig@uv.es.

<sup>5</sup> The abbreviations used are: ARE, AU-rich element; BPS, bathophenanthroline disulfonic acid; GAD, Gal4 activation domain; GBD, Gal4 DNA-binding domain; GFP, green fluorescent protein; P-body, processing body; RFP, red fluorescent protein; TTP, tristetraprolin; TZF, tandem zinc finger; UTR, untranslated region.

## Mechanism of Cth2-mediated mRNA Decay

degradation by a large complex of exonucleases known as the exosome. Alternatively, the 5' cap structure can be removed by the decapping enzyme complex Dcp1/Dcp2, followed by 5' to 3' digestion of the transcript body by the Xrn1 cytoplasmic exonuclease.

The conserved Dhh1/RCK/p54 protein, which functions as an activator of decapping, plays a critical function in modulating and connecting mRNA translation and turnover (14, 15). The recent elucidation of Dhh1 crystal structure has revealed that, like other previously characterized DEAD box proteins, Dhh1 contains two RecA-like  $\alpha/\beta$  domains (14), referred to as the amino-terminal (Dhh1-Nt) and carboxyl-terminal (Dhh1-Ct) domains. The Dhh1-Nt domain contains ATP-binding and hydrolysis motifs, whereas the Dhh1-Ct domain exhibits motifs associated with RNA binding (14). The structure of Dhh1 and the functional analysis of different Dhh1 mutants indicate that ATP and RNA binding induce a conformational change that leads to a more compact structure with extensive interactions between the Dhh1-Nt and Dhh1-Ct domains (14). Importantly, the Dhh1-Ct domain physically interacts with the Dcp1/Dcp2 decapping complex and the Edc3 scaffold protein, thereby promoting the transition of mRNAs from translation to decapping and 5' to 3' degradation at specific intracellular sites known as processing bodies (P-bodies) (15–17).

P-bodies are cytosolic foci containing translationally repressed mRNAs, which can be either degraded or stored, associated with the translation repression and mRNA decay machinery. Conserved core proteins of P-bodies include Dcp1/Dcp2, Dhh1, Edc3, Xrn1, the translation repressor Pat1 and the heptameric Lsm1–7 complex. The cross-bridging protein Edc3 and the “prion-like” domain in Lsm4 mediate the aggregation of individual mRNPs into larger P-body assemblies (17). It has been proposed that the assembly of the general repression/decay complexes in P-bodies is in competition with the assembly of translational factors (reviewed in Refs. 18 and 19). P-bodies are therefore highly dynamic structures with mRNAs and proteins rapidly cycling in and out (20). Inhibition of mRNA decay at late stages (*xrn1* $\Delta$ , *dcp1* $\Delta$ , *dcp2* $\Delta$ , and *lsm1* $\Delta$  mutants) or blockage of translation initiation (glucose deprivation and osmotic stress) dramatically increases the number and size of P-bodies, whereas an inhibition of mRNA turnover at earlier steps (*ccr4* $\Delta$ , *pop2* $\Delta$ , *dhh1* $\Delta$  and *pat1* $\Delta$  mutants) traps mRNAs in polysomes and decreases visible P-bodies (15, 16, 21, 22). Multiple proteins that participate at different levels in the post-transcriptional regulation of mRNA expression, including proteins involved in non-sense-mediated decay or proteins that regulate subclasses of mRNAs, rapidly transit through P-bodies and only accumulate at detectable levels in certain mutant backgrounds, when overexpressed or under stressful conditions (reviewed in Refs. 18 and 19).

Recent results have shown that some mRNA-specific regulatory proteins recruit the general repression and decay machinery to specific transcripts. In yeast, the PUF family member protein Mpt5 interacts with the Pop2 deadenylase, thereby inducing the recruitment of the Ccr4, Dhh1, and Dcp2 proteins to individual mRNAs to promote mRNA deadenylation and decay (23). Human tristetraprolin (TTP), a well characterized member of the family of proteins containing TZF of the

CX<sub>8</sub>CX<sub>5</sub>CX<sub>3</sub>H-type, promotes the rapid decay of some ARE-containing mRNAs encoding for cytokines and interleukins (reviewed in Ref. 24). The identification of mRNA decay factors that associate with TTP and different mRNA decay assays suggests that TTP promotes mRNA turnover by recruiting the mRNA decay enzymes responsible for deadenylation, decapping, and 5' to 3' turnover, as well as 3' to 5' exonucleolytic degradation (25–30). An unresolved issue is the diversity of interactions that allow mRNA specific-binding proteins to recruit the mRNA degradation machinery.

In this report, we provide novel information on the post-transcriptional regulatory mechanisms that control the adaptation of eukaryotic cells to iron deficiency. Despite the important function played in yeast by the RNA-binding proteins Cth1 and Cth2 in this process, their mechanism for targeted mRNA degradation is currently unknown. Here, we provide genetic and molecular evidence, including mRNA decay assays and protein-protein interaction experiments, that point to a function for the DEAD box Dhh1 helicase in the mechanism of Cth2-mediated mRNA decay. Furthermore, the analysis of trapped intermediates during mRNA degradation and the localization of Cth2 protein to P-bodies in specific mRNA decay mutants suggest that, in response to iron deficiency, Cth2 promotes mRNA by the 5' to 3' decay pathway. These results contribute to further understand the multiple mechanisms underlying the post-transcriptional regulation of ARE-containing mRNAs in eukaryotic cells.

## EXPERIMENTAL PROCEDURES

**Yeast Strains and Growth Conditions**—Genotypes for the yeast strains used in this work are listed in supplemental Table S1. To test the effect of *CTH2* overexpression on yeast growth rate, cells were grown on SC-ura (synthetic medium without uracil and containing 2% glucose) to exponential phase ( $\sim A_{600} = 0.3$ – $0.6$ ), washed, and spotted in 10-fold serial dilutions starting at  $A_{600} = 0.1$  on SC-ura and SCGal-ura (SC without uracil, without glucose, and containing 2% galactose), and incubated at 30 °C for 3–4 days. For yeast two-hybrid assays, AH109 cells co-transformed with GAD- and GBD-based plasmids were grown in SC-leu-trp (SC without leucine and tryptophan) to exponential phase and spotted in 10-fold serial dilutions on SC-leu-trp (+His), SC-leu-trp-his (SC without leucine, tryptophan, and histidine) with 3-amino-1,2,4-triazole (–His), and SC-adenine, and incubated at 30 °C for 3–5 days.

**Plasmids**—Plasmids used in this study are listed in supplemental Table S2. The coding sequences from wild type *CTH2* and *CTH2-C190R* were cloned into the p416GAL vector using standard cloning methods. The pRS416-*CTH2-C190R* plasmid (10) was used as a template for *CTH2-C190R* PCR amplification. The entire coding region of *DHHL1*, the amino-terminal *DHHL1* region (amino acid residues 1–248), and the carboxyl-terminal *DHHL1* region (amino acid residues 249–507) were cloned in frame with the Gal4 DNA-binding domain of the pGBK-T7 plasmid (Matchmaker, BD Biosciences), generating the pGBK-DHHL1, pGBK-DHHL1-Nt, and pGBK-DHHL1-Ct plasmids, respectively. The *CTH1* coding region was cloned in frame with the Gal4-activating domain of the pGAD-T7 plas-

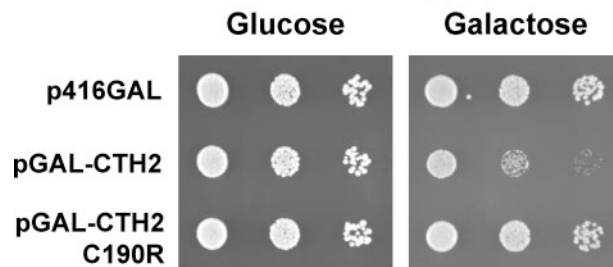
mid (BD Biosciences) generating the pGAD-CTH1 plasmid. The p416GAL-SDH4pG plasmid was obtained in two steps; first, 218 nucleotides from the *SDH4* 3'-UTR were PCR-amplified and cloned into the pRS416 vector (the poly(G) track was included within the forward oligonucleotide), and second, a fragment containing the *GAL1* promoter and the *SDH4* coding sequence from p416GAL-SDH4 plasmid was cloned in. GFP was introduced in frame after the *CTH2* start codon of pRS416-CTH2 plasmid (10) to generate pRS416-GFP-CTH2. All of the PCR amplifications were performed with the Expand High Fidelity PCR System (Roche Applied Science), and plasmids were verified by sequencing.

**RNA Isolation and Analysis in Agarose Gels**—For steady-state mRNA analysis (see Fig. 2A), the cells were grown in SC-ura-leu (SC lacking uracil and leucine) containing 100  $\mu\text{M}$   $\text{Fe}(\text{NH}_4)_2(\text{SO}_4)_2$  (+Fe) or 100  $\mu\text{M}$  of the iron chelator bathophenanthroline disulfonic acid or BPS (−Fe) to exponential phase. For half-life measurements, the cells were grown overnight in SCraf-ura-leu (no glucose and 2% raffinose) and reinoculated in the same medium containing 100  $\mu\text{M}$   $\text{Fe}(\text{NH}_4)_2(\text{SO}_4)_2$  (+Fe) or 100  $\mu\text{M}$  BPS (−Fe) to exponential phase. Galactose was added at a final concentration of 4% for 2 h. Finally, 4% glucose was added to terminate transcription of *SDH4* mRNA. Aliquots were isolated before galactose addition, and at 0, 2, 4, 6, 8, 10, 15, and 20 min after transcription shut-off. Total yeast RNA was isolated with a modified hot phenol method and analyzed on a 1.5% formaldehyde agarose gel as previously described (10). PCR-amplified fragments were gel-purified and radiolabeled with [ $^{32}\text{P}$ ]dCTP to be used as probes. The samples were analyzed by RNA blotting with *SDH4* and *ACT1* probes and quantified with a FLA-3000R phosphorimaging device (Fujifilm). *SDH4* values were normalized with *ACT1* values. The half-life was determined as the average of at least three independent experiments, and standard deviation was calculated.

**RNA Isolation and Analysis in Polyacrylamide Gels**—The cells were grown in SC-ura-leu containing 100  $\mu\text{M}$   $\text{Fe}(\text{NH}_4)_2(\text{SO}_4)_2$  (+Fe) or 100  $\mu\text{M}$  BPS (−Fe) to the exponential phase. Total yeast RNA was isolated and analyzed on 6% polyacrylamide, 7.5 M urea gels as described (31). The *SDH4*:437R (5'-AAAGGGAGACCGCAGAACCAAG-3') oligonucleotide and oligo(dT) were used for RNase H digestions. End-labeled *SDH4*cds (5'-GTCTTTCTCGGAAGAATCCCA-3') and *SDH4*-3UTR (5'-GATGTGCATGTTACATGACCGA-3') oligonucleotides were used as *SDH4* probes, upstream and downstream of the poly(G) track, respectively; and the oRP100 oligonucleotide was used as a probe for the *SCR1* loading control. The images were obtained with a Molecular Dynamics (Sunnyvale, CA) phosphorimaging device.

**Fluorescence Microscopy**—For GFP-Cth2 and Dcp2-RFP subcellular localization, the cells were grown in selective medium with 100  $\mu\text{M}$  BPS to early exponential phase ( $A_{600} = 0.3$ – $0.4$ ). The images were acquired with a Nikon PCM 2000 confocal microscope (Melville, NY) using a 100 $\times$  objective with a 3 $\times$  zoom using Compix software (Sewickley, PA). The images in Fig. 5A are a z-series compilation of 6–10 images in a stack. Co-localization experiments (see Fig. 5B) are made from a single z-plane image.

## Wild type



## dhh1Δ

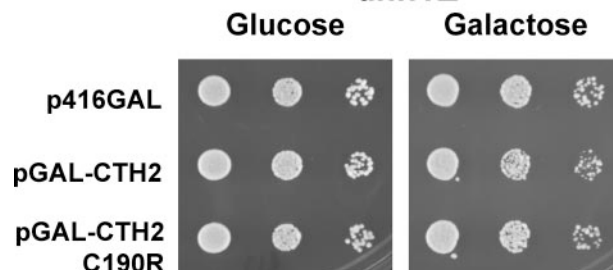


FIGURE 1. Growth impairment caused by *CTH2* overexpression is rescued in *dhh1Δ* mutant cells. Wild type BY4741 and *dhh1Δ* cells transformed with p416GAL, p416GAL-CTH2 (pGAL-CTH2), and p416GAL-CTH2-C190R (pGAL-CTH2-C190R) were assayed for growth on SC-ura (Glucose) and SCGal-ura (Galactose) media.

## RESULTS

**Deletion of DHH1 Rescues Growth Impairment Caused by CTH2 Overexpression**—In response to iron deficiency, the yeast mRNA-binding proteins Cth1 and Cth2 promote the coordinated degradation of a group of mRNAs that lead to a genome-wide reprogramming of iron-dependent metabolism (10, 11). The transcription of both genes is induced by the iron-regulated transcription factors Aft1 and Aft2 (7, 10, 11, 32). Although Cth2 protein is undetectable under iron-sufficient conditions and highly expressed upon iron starvation, Cth1 protein levels are low but transiently induced during iron deficiency (10, 11). Previous results have shown that overexpression of Cth1 or Cth2 proteins under iron-sufficient conditions impairs cell growth (33). Furthermore, deletion of a region containing the  $\text{CX}_8\text{CX}_5\text{CX}_3\text{H}$  TZF motif within Cth1 protein rescues cell growth to wild type rates (33). To reproduce these observations, we have cloned the *CTH2* coding sequence under the control of the glucose-repressible and galactose-inducible *GAL1* promoter (pGAL-CTH2 plasmid). As expected, no difference in growth rate is observed between wild type cells transformed with pGAL-CTH2 and p416GAL empty vector when grown on glucose-containing medium, whereas a significant growth defect is observed for wild type cells expressing pGAL-CTH2 in galactose-containing medium (Fig. 1). We have previously reported that mutagenesis of a single cysteine residue (C190R) within Cth2 TZF motif severely reduces RNA binding and degradation of Cth2 mRNA targets (10). Overexpression of the *CTH2*-C190R mutant allele under the control of the *GAL1* promoter does not induce growth defects on galactose-containing medium as compared with wild type cells harboring empty vector (Fig. 1). These results strongly suggest that

## Mechanism of Cth2-mediated mRNA Decay

impaired growth caused by *CTH2* overexpression is a consequence of specific binding of the Cth2 protein to target mRNAs.

With the aim to identify proteins that might be required for the mechanism of Cth2-mediated mRNA degradation, we have assayed the effect of *CTH2* overexpression on the growth rate of yeast strains lacking proteins previously shown to be involved in mRNA turnover. Single deletions in the *POP2* and *PAN2* deadenylases; *EDC1*, *EDC2*, and *EDC3* decapping enhancers; *PAT1* and *LSM1* translation regulators; *XRN1* 5'-3' exonuclease; the *SKI2* cytosolic subunit of the exosome; and the *RRP6* nuclear subunit of the exosome exhibited growth impairment when *CTH2* was overexpressed, as previously shown for wild type cells (data not shown). Importantly, deletion of the DEAD box RNA helicase *DHH1* rescued cell growth impairment caused by *CTH2* overexpression (Fig. 1), suggesting that Dhh1 protein plays a role in the mechanism of Cth2-mediated mRNA turnover.

**Dhh1 Is Required for the Degradation of *SDH4* mRNA in Iron-deficient Conditions**—We have previously described that Cth2 protein specifically binds to AREs within the 3'-UTR of *SDH4* mRNA and promotes its specific degradation in response to iron starvation (10). With the aim to ascertain the function of Dhh1 RNA-helicase in the mechanism of Cth2-induced turnover upon iron starvation, we have determined the steady-state mRNA levels of *SDH4* mRNA in wild type *CTH2*, *cth2Δ*, and *dhh1Δ* cells, growth under iron-sufficient (+Fe) and iron-deficient (−Fe) conditions. Given the partially overlapping function of Cth1 and Cth2 proteins in mRNA degradation (11), we have performed these experiments in cells lacking the *CTH1* gene (*cth1Δ* background). As previously described, steady-state *SDH4* mRNA levels decrease in wild type *CTH2* cells grown under iron-deficient conditions, whereas no mRNA down-regulation is observed in *cth2Δ* cells (Fig. 2A and Ref. 10). *dhh1Δ* mutant cells grown under iron-sufficient conditions do not display any significant change in *SDH4* mRNA levels with respect to wild type and *cth2Δ* mutant cells; and more importantly, *SDH4* mRNA levels do not decrease under iron-deficient conditions (Fig. 2A). Because *CTH2* induction by iron deficiency is not affected in *dhh1Δ* mutant cells (Fig. 2A), these results indicate that Dhh1 is required for the down-regulation of *SDH4* mRNA upon iron limitation.

To further investigate the function of Dhh1 protein in the post-transcriptional regulation of *SDH4* mRNA, we have determined *SDH4* mRNA half-life under iron-sufficient and iron-deficient conditions in *dhh1Δ* mutant cells as compared with wild type *CTH2* and *cth2Δ* cells. Again, *CTH1* gene has been deleted from these strains to avoid any overlapping effect with *CTH2* function. The *SDH4* coding sequence and 3'-UTR have been conditionally expressed with the *GAL1* promoter. The cells were transiently grown in galactose to induce the expression of *SDH4* mRNA, and glucose was added to shut off *SDH4* transcription. The samples were processed and analyzed to determine *SDH4* mRNA levels at different time points. As previously described (10), wild type *CTH2* cells grown under iron-sufficient conditions exhibit a longer *SDH4* mRNA half-life than cells grown under iron-deficient conditions (Fig. 2, B and C, 14.5 versus 8.3 min). No significant change in *SDH4* mRNA half-life is observed for *cth2Δ* cells grown under plus and minus

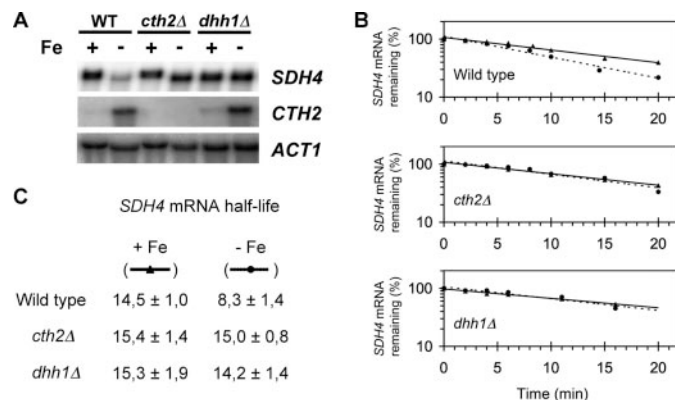


**FIGURE 2. The degradation of *SDH4* mRNA in iron-deficient conditions depends on *DHH1*.** A, steady-state *SDH4* mRNA levels. *cth1Δcth2Δsdh4Δ* cells co-transformed with pRS415-*CTH2* plus pRS416-*SDH4* plasmids (wild type (WT)) or pRS415 plus pRS416-*SDH4* plasmids (*cth2Δ*), and *cth1Δcth2Δsdh4Δdhh1Δ* cells co-transformed with pRS415-*CTH2* plus pRS416-*SDH4* plasmids (*dhh1Δ*) were grown in SC-ura-leu medium containing 100  $\mu$ M iron (+Fe) or 100  $\mu$ M BPS (−Fe), RNA extracted, and analyzed by RNA blotting. B, *SDH4* mRNA half-life. *cth1Δcth2Δsdh4Δ* cells were co-transformed with either pRS416-*CTH2* plus p415GAL-*SDH4* plasmids (wild type), or pRS416 plus p425GAL-*SDH4* plasmids (*cth2Δ*), and *cth1Δcth2Δsdh4Δdhh1Δ* cells were co-transformed with pRS416-*CTH2* plus p415GAL-*SDH4* plasmids (*dhh1Δ*). Transformants were grown under iron deficiency (−Fe, dotted line and black circles) or iron sufficiency (+Fe, solid line and black triangles) to exponential phase. Galactose was added to induce and glucose was added to stop *SDH4* transcription. Total RNA was extracted and analyzed by RNA blotting. The data points from a representative experiment are shown. C, mRNA half-lives were calculated on the basis of at least three independent experiments, and standard deviation is represented. *ACT1* mRNA was used as a loading control.

iron conditions (Fig. 2, B and C, 15.4 versus 15.0 min) (10). *dhh1Δ* cells grown under iron sufficiency showed a half-life of 15.3 min, which is similar to the values obtained for wild type *CTH2* and *cth2Δ* cells under iron sufficiency (Fig. 2, B and C). *SDH4* mRNA half-life did not significantly decrease in *dhh1Δ* mutants when *CTH2* expression was induced by growth under iron deficiency (Fig. 2, B and C, 14.2 min), suggesting that *DHH1* is important for the regulation of *SDH4* mRNA stability during iron scarcity. Taken together, these results are consistent with a function of Dhh1 protein in the mechanism of *SDH4* mRNA turnover in response to iron deprivation.

**Cth2 Protein Interacts *In Vivo* with the Carboxyl-terminal Domain of Dhh1 Protein**—The rescue of *CTH2* overexpression toxicity by *dhh1Δ* mutant cells (Fig. 1) and the lack of *SDH4* mRNA degradation upon iron deficiency in *dhh1Δ* mutants (Fig. 2) prompted us to postulate a model for the function of Dhh1 in the mechanism of Cth2-mediated mRNA turnover. Binding of Cth2 protein to ARE-containing mRNAs, in response to iron deficiency, could induce the recruitment of Dhh1 protein to specific Cth2 mRNA targets and thus promote their degradation by the general machinery for mRNA turnover. To test this hypothesis, we assayed the *in vivo* interaction between Cth2 and Dhh1 proteins using the yeast two-hybrid system. For this purpose, the full-length coding sequence of *DHH1* was fused in-frame to the GBD and *CTH2* coding sequence to GAD (10). If both proteins interact *in vivo*, the transcription of the *HIS3* reporter gene within the *his3*-deficient AH109 host strain will be activated, and the cells will grow in the absence of histidine (−His). As shown in Fig. 3 (upper panels), cells co-expressing GBD-Dhh1 and GAD-Cth2

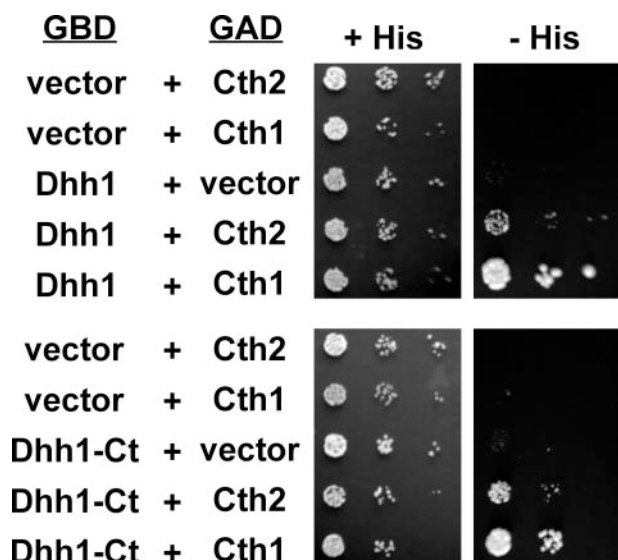


**FIGURE 3. Cth1 and Cth2 proteins interact with the carboxyl-terminal domain of Dhh1.** Yeast two-hybrid assay between Cth1/Cth2 proteins and Dhh1. AH109 cells containing either pGBK-T7 (GBD-vector), pGBK-DHH1 (Dhh1, upper panels) or pGBK-DHH1-Ct (Dhh1-Ct, bottom panels) were transformed with pGAD-T7 (GAD-vector), pGAD-CTH1 (Cth1), or pGAD-CTH2 (Cth2) and spotted on SC-leu-trp (+His) and SC-leu-trp-his with 3-aminotriazol (-His).

(Dhh1 + Cth2) grow in minus histidine, whereas cells expressing GBD-Dhh1 (Dhh1 + vector) or GAD-Cth2 (vector + Cth2) separately do not grow in these conditions, indicating that Dhh1 and Cth2 proteins interact *in vivo*. Similar results were obtained when cells were assayed in medium without adenine, another reporter gene available for the assay (data not shown). We have previously shown that Cth1 protein contributes to the global metabolic remodeling in response to iron deficiency by binding and inducing the turnover of many ARE-containing mRNAs (11). Because Cth1 protein exhibits 56% amino acid similarity to Cth2, we assayed its interaction with Dhh1 protein. A fusion of *CTH1* coding sequence to the GAD also displayed interaction with GBD-Dhh1 (Fig. 3, *Cth1* lanes), strongly suggesting that both TZF-containing proteins interact *in vivo* with the Dhh1 helicase.

Because Dhh1 protein harbors two characterized functional domains (14), we carried out experiments to identify the region within Dhh1 responsible for its interaction with Cth1 and Cth2. For this purpose, we separately fused Dhh1-Nt (amino acid residues 1–248) and Dhh1-Ct (amino acid residues 249–507) to the GBD and assayed their interaction with Cth1 and Cth2 by yeast two-hybrid. Cells co-expressing Dhh1-Ct and Cth2 (or Cth1) proteins show growth rates in the absence of histidine similar to those obtained for full-length Dhh1 (Fig. 3, bottom panels, *Dhh1-Ct*), whereas Dhh1-Nt-expressing cells do not display growth under these conditions (data not shown). Taken together, these results strongly suggest that the Cth1 and Cth2 proteins recruit the DEAD box RNA helicase Dhh1 by interacting with its carboxyl-terminal domain.

**Cth2 Promotes the 5' to 3' Degradation of *SDH4* mRNA**—The Dhh1 helicase plays an important function in the early stages of the 5' to 3' mRNA decay pathway by interacting with the catalytic domain of Dcp2 decapping enzyme (15, 17). Therefore, our model for a function of Dhh1 in the mechanism of Cth2-

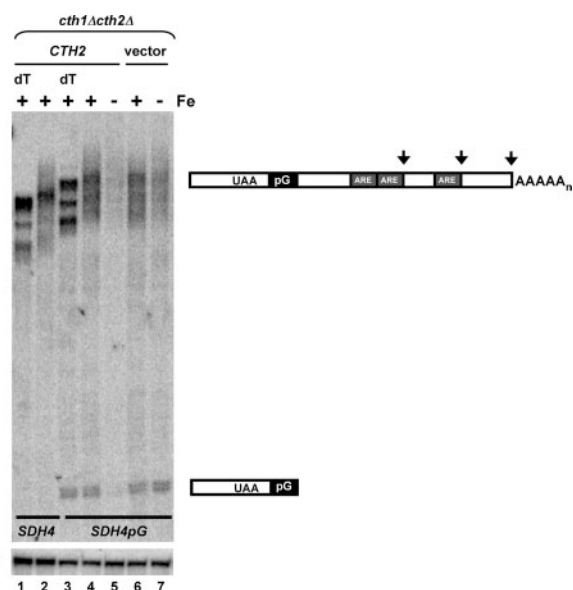


**FIGURE 4. Cth2 induces the degradation of *SDH4* mRNA by the 5' to 3' decay pathway.** *cth1Δcth2Δsdh4Δ* cells co-transformed with pRS415-CTH2 plus pRS416-*SDH4* plasmids (wild type, *SDH4*), or pRS415-CTH2 plus pRS416-*SDH4pG* plasmids (wild type, *SDH4pG*), and *cth1Δcth2Δsdh4Δ* cells co-transformed with pRS415 plus pRS416-*SDH4pG* plasmids (*cth2Δ*) were grown in SC-ura-leu media containing 100  $\mu$ M iron (+Fe) or 100  $\mu$ M BPS (-Fe) to exponential phase. Total RNA was extracted, digested with RNase H before loading, and RNA blot hybridized to the end-labeled *SDH4*:437R oligonucleotide. Polyadenylation sites on *SDH4* transcript (vertical arrows) were determined from samples treated with oligo(dT) and RNase H samples (dT, lanes 1 and 3). The samples were analyzed by PAGE and RNA blotting with an end-labeled *SDH4*cds oligonucleotide. *SCR1* RNA is shown as a loading control. The relative positions of *SDH4* termination codon (UAA), poly(G) track (pG), and ARE have been represented. Migration of full-length *SDH4* mRNA and the poly(G) decay intermediate is indicated.

mediated mRNA turnover predicts that, in response to iron deficiency, Cth2 should induce the degradation of *SDH4* transcript via the 5' to 3' mRNA decay pathway. To ascertain the directionality of *SDH4* mRNA degradation induced by Cth2 in response to iron deprivation, we introduced within *SDH4* 3'-UTR a poly(G) track containing 18 guanylate residues, which is expected to fold in a strong secondary RNA structure that blocks the exonucleolytic digestion of mRNAs (31). The decay of *SDH4pG* mRNA upon iron scarcity does not differ from the wild type *SDH4* allele, indicating that its regulation by iron availability is not altered (data not shown). We analyzed the *SDH4pG* and *SDH4* transcripts expressed in wild type *CTH2* cells (*cth1Δ* background) grown under iron-sufficient conditions by polyacrylamide RNA blotting (Fig. 4, lanes 1–4). Before loading, all of the RNA samples were hybridized to a reverse oligonucleotide located 129 nucleotides upstream the *SDH4* termination codon and then cleaved with RNase H to decrease the final size of the transcripts. Furthermore, with the aim to determine the *SDH4* polyadenylation sites as compared with *SDH4pG* allele, some RNA samples were hybridized with oligo(dT) before RNase H treatment to remove the poly(A) tail (Fig. 4, lanes 1 and 3). Hybridization with an end-labeled oligonucleotide probe within *SDH4* coding sequence, and therefore located upstream of the poly(G) tract, shows three major *SDH4* polyadenylation sites (Fig. 4, lane 1). The *SDH4pG* transcript exhibits the expected increase in size, and it conserves the predominant polyadenylation sites (Fig. 4, lane 3). In addition, an

## Mechanism of Cth2-mediated mRNA Decay

mRNA decay intermediate (~160 nucleotides), consistent with a 3' to poly(G) track degradation and the accumulation of a 5' to poly(G) fragment, is trapped for the *SDH4pG* allele (Fig. 4, lanes 3 and 4). No trapped mRNA decay intermediates are observed for the wild type *SDH4* allele (Fig. 4, lanes 1 and 2) or when an oligonucleotide probe hybridizing downstream of the poly(G) track is used (supplemental Fig. S1), suggesting that *SDH4pG* allele is preferentially degraded by a 3' to 5' degradation pathway under iron-sufficient conditions.

We also observed that growth under iron-deficient conditions promotes the down-regulation of full-length *SDH4pG* mRNA levels in a *CTH2*-dependent manner, and more importantly, the complete removal of the 5'-poly(G) trapped intermediate, which can only be degraded by exonucleases from its 5' end (Fig. 4, lanes 5–7). The loss of the 5'-poly(G) intermediate during iron deficiency is inconsistent with *CTH2* enhancing the 3' to 5' degradation of the *SDH4* mRNA, which would be expected to lead to an increase in this fragment. On the other hand, we do not detect a 5' to 3' degradation intermediate produced form of the *SDH4* mRNA, perhaps because the poly(G) tract is inefficient at blocking Xrn1 in this mRNA. However, we observe that when inserted into the MFA2pG mRNA, the *SDH4* AREs can lead to the formation of a mRNA trapped fragment produced by 5' to 3' degradation under iron-deficient conditions (supplemental Fig. S2). Taken together these results argue that Cth2 promotes 5' to 3' degradation of the *SDH4* mRNA.

**Cth2 Protein Localizes to P-bodies in Strains Defective in 5' to 3' mRNA Turnover**—Our data strongly suggest that the mechanism for Cth2-mediated degradation of *SDH4* mRNA under iron-deficient conditions involves the recruitment of the Dhh1 RNA helicase. Dhh1 protein interacts with multiple members of the general machinery of mRNA decay, and it promotes the 5' to 3' degradation of mRNAs at cytoplasmic P-bodies (15, 17). These observations suggest that Cth2 protein might, at least transiently, localize to P-bodies, where *SDH4* mRNA degradation would occur. To test this hypothesis, we epitope-tagged the Cth2 protein at its amino-terminal end with the GFP, keeping the *CTH2* native promoter region to express endogenous levels of Cth2 protein upon iron deprivation. We first studied the dynamics of P-body assembly under iron-deficient conditions by localizing Dcp2-GFP protein, a core component of P-bodies, in multiple conditions and strains. No significant difference in Dcp2-GFP distribution and P-body assembly between cells grown under iron-deficient and iron-sufficient conditions is observed (data not shown). Under iron deficiency, exponentially growing wild type cells show an even distribution throughout the cell for the fully functional GFP-Cth2 fusion protein (Fig. 5A, WT), whereas no fluorescence is observed under iron-sufficient conditions (data not shown). The Xrn1 exonuclease and the Dcp1/Dcp2 decapping enzymes are essential for the 5' to 3' pathway of mRNA decay (reviewed in Ref. 12 and 13). Yeast strains defective in any of these proteins accumulate elevated levels of mRNAs targeted for degradation, which cause an increase in the number and size of cytosolic P-bodies in both iron-sufficient and iron-deficient conditions (Fig. 5B and Ref. 16, 22). We observe that the GFP-Cth2 protein is trapped in cytoplasmic foci resembling P-bodies, when

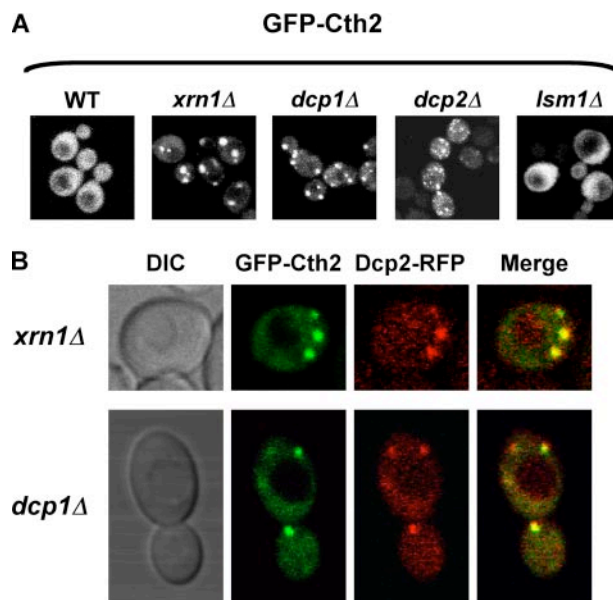


**FIGURE 5. Cth2 protein is trapped within processing-bodies in *xrn1Δ*, *dcp1Δ*, and *dcp2Δ* mutant cells.** A, localization of GFP-Cth2 in wild type BY4741 (WT), *xrn1Δ*, *dcp1Δ*, *dcp2Δ*, and *lsm1Δ* strains. The cells were transformed with pRS416-GFP-CTH2 and grown in SC-ura to early exponential growth phase. B, co-localization of GFP-Cth2 and RFP-Dcp2 in *xrn1Δ* and *dcp1Δ* mutants. The cells were co-transformed with pRS416-GFP-CTH2 and RFP-Dcp2 plasmids and grown in SC-ura-leu to early exponential growth phase. DIC, differential interference microscopy.

expressed in *xrn1Δ*, *dcp1Δ*, and *dcp2Δ* mutant cells (Fig. 5A). To further investigate the nature of these cytoplasmic foci, we performed co-localization assays with Dcp2 protein epitope-tagged with the RFP. As shown in Fig. 5B, GFP-Cth2 and Dcp2-RFP proteins co-localize in both *xrn1Δ* and *dcp1Δ* mutants grown under iron-deficient conditions. These results demonstrate that Cth2 protein accumulates within P-bodies in *xrn1Δ*, *dcp1Δ*, and *dcp2Δ* cells, which is consistent with Cth2 acting by recruiting the general machinery for deadenylation and 5' to 3' mRNA degradation.

In yeast, Dhh1 and Pat1 proteins independently repress translation by activating mRNA decapping (15). Although overexpression of *DHH1* or *PAT1* promotes the accumulation of P-bodies, deletion of these genes diminishes the flux of untranslated mRNAs toward repression, causing a decrease in P-body assembly. Therefore, exponentially growing *dhh1Δ* and *pat1Δ* mutant cells do not contain any visible P-bodies under iron-sufficient and iron-deficient conditions (Refs. 16 and 22 and data not shown). Cells defective on the major Ccr4/Pop2/Not deadenylase or in the cytosolic Ski subunits of the exosome also lack any visible P-bodies at early exponential growth phase (Refs. 16 and 22 and data not shown). As expected, the GFP-Cth2 protein does not localize to cytoplasmic foci in any of these strains (supplemental Fig. S3).

The Lsm1–7 complex, which is recruited to P-bodies by Pat1 protein, functions in a rate-limiting step of decapping occurring after P-body assembly (22). Therefore, at the early exponential growth phase, *lsm1Δ* cells exhibit a dramatic increase in the number of P-bodies within the cytoplasm, in both iron-sufficient and iron-deficient conditions, as compared with wild type cells (Ref. 22 and data not shown). GFP-Cth2 protein does not accumulate in P-bodies in exponentially growing *lsm1Δ*

cells but maintains a distribution throughout the cell similar to the pattern observed for wild type cells (Fig. 5A, *lsm1Δ*). Finally, we observe that conditions that normally promote a dramatic increase in the assembly of P-bodies, such as glucose deprivation, osmotic stress, and stationary phase, do not cause any accumulation of Cth2 at P-bodies, indicating that the mere presence of these aggregates within the cell does not trigger Cth2 trapping (data not shown). Taken together, these results illustrate the dynamics of Cth2 subcellular localization, demonstrating that the function of Xrn1, Dcp1, and Dcp2 proteins, but not Lsm1, is essential for the exit of Cth2 protein from P-bodies. Furthermore, the results strongly suggest that the components of the 5' to 3' mRNA degradation machinery Xrn1, Dcp1, and Dcp2 participate in the mechanism of Cth2-mediated mRNA turnover.

## DISCUSSION

Eukaryotic cells have developed multiple strategies to efficiently respond to fluctuations in iron availability (2, 3, 6). Upon iron deficiency, the *S. cerevisiae* Cth1 and Cth2 proteins cooperate to promote remodeling of iron metabolism by inducing the coordinated degradation of many mRNAs encoding proteins that function in iron-dependent pathways (10, 11). Cth1 and Cth2 proteins bind to AREs within the 3'-UTR of target mRNAs, and they induce mRNA decay by an uncharacterized mechanism (10, 11). Several reasons have prompted us to investigate the mechanisms of mRNA turnover induced by Cth1/2 proteins. First, Cth1 and Cth2 play crucial functions in the adaptation of cells to iron deficiency; second, despite AREs being the best characterized mRNA instability elements in eukaryotic cells, the mechanisms underlying its regulation by ARE-binding proteins are poorly understood; and third, *S. cerevisiae* has contributed enormously to the elucidation of the general pathways of mRNA decay in eukaryotes and constitutes an excellent model organism for these studies. In this report, we have focused on Cth2 protein because its expression is dramatically induced upon iron starvation, and its deletion or mutation within the TZF motif causes a severe growth defect on iron-deficient medium, as compared with Cth1 (10, 11).

We had observed that overexpression of Cth2 protein at levels above those provided by its native iron-regulated promoter or by a highly expressed constitutive promoter caused cell growth impairment.<sup>6</sup> Therefore, we took advantage of a yeast genetic assay to identify genes implicated in the mRNA turnover mediated by Cth2. Conditional overexpression of *CTH2* with the *GAL1* promoter causes a significant growth defect to wild type cells (Fig. 1 and Ref. 33). However, the molecular reason by which *CTH2* overexpression causes growth impairment is not known. One possibility is that overexpression of Cth2 titrates out specific proteins and limits their availability to the cell. Alternatively, increasing *CTH2* levels could accelerate in excess the degradation of important mRNAs. In any case, *CTH2* toxicity is a consequence of its specific function in mRNA binding and degradation, given that overexpression of the *CTH2-C190R*

mutant allele in wild type cells does not impair growth. Thus, we propose that the deletion of *DHH1* restores the growth of *CTH2*-overexpressing cells by either inhibiting the degradation of specific Cth2 targets or by preventing the sequestration of important proteins.

The DEAD box Dhh1 helicase promotes the transition of mRNAs from the pool undergoing active translation to cytoplasmic P-bodies, where decapping and 5' to 3' degradation takes place, by physically interacting with the Dcp2/Dcp1 decapping complex and the Edc3 protein (15, 17). These data and the interaction we have observed between the Cth2 and Dhh1 proteins prompt us to postulate that Cth2 could recruit the Dcp1-Dcp2-Edc3-Dhh1 protein complex to a specific set of ARE-containing mRNAs. The recruitment of members of the general machinery of mRNA decay to coordinately modulate the expression of a group of genes has been proposed for other mRNA-specific regulatory proteins. In yeast, Mpt5, a PUF family member protein, directly interacts with the Pop2 protein, which functions as a bridge to recruit Ccr4, Dcp1, and Dhh1 proteins to specific target mRNAs to repress translation and stimulate deadenylation and mRNA decay (23, 34). We should note that in the case of the mechanism of Cth2-mediated degradation, a single region in Dhh1 protein, its carboxyl-terminal domain is responsible for the interaction with Dcp2, Edc3, and Cth2 proteins, which raises the question of whether these interactions can all occur simultaneously.

In humans, the TZF-containing protein TTP associates with multiple components of the mRNA decay machinery including the hCcr4 deadenylase, the exosome components hRrp4 and PM-Scl75, the decapping enzymes hDcp2/hDcp1 and hEdc3, and the exonuclease hXrn1 (26–29). These data and additional RNA decay assays indicate that TTP promotes the decay of ARE-containing mRNAs by multiple mechanisms requiring deadenylation, decapping, and both 5' to 3' and 3' to 5' exonucleolytic decay. Although the preferential mechanism has not been demonstrated, recent data, including mRNA decay and localization experiments, point to the 5' to 3' degradation as the primary mRNA decay pathway for ARE-containing mRNAs in human cells (30, 35). Furthermore, elegant experiments have demonstrated that, similarly to transcription factors, TTP contains, in addition to the RNA-binding domain, two regions that function as mRNA decay activation domains (26). It should be noted that the similarity between the families of proteins containing TZF motifs from different organisms including humans, budding and fission yeasts, worms, and plants is restricted to the TZF region.<sup>6</sup> Regions outside the RNA-binding motif, which would harbor the mRNA decay activation domains, differ considerably between TZF-containing proteins from different species, indicating that the mechanism for mRNA decay may be different. Within a single organism, the putative RNA activation domains in TZF-containing proteins exhibit a higher similarity, suggesting that they could mediate mRNA decay by recruiting the same degradation factors (supplemental Fig. S4 for a phylogenetic analysis). In mammals, the TTP homologue protein BRF1 exhibits a pattern of interaction with mRNA decay factors similar to TTP (26).

<sup>6</sup> S. Puig, unpublished observations.

## Mechanism of Cth2-mediated mRNA Decay

In yeast, the interaction between Cth1/2 and Dhh1 shown here and the previously described connection between the yeast Dcp1-Dcp2-Edc3-Dhh1 and Pat1-Lsm1-7-Xrn1 subcomplexes (36) strongly suggest that the degradation of Cth1/2 targets occurs by the 5' to 3' mRNA decay pathway. Consistent with this hypothesis, the degradation of trapped *SDH4* intermediates containing a poly(G) track at its 3' end, which can only occur via the 5' to 3' pathway, is enhanced in wild type but not *cth2Δ* cells when grown under iron starvation conditions (Fig. 4). Further experiments will be required to ascertain whether the Cth1 and Cth2 mechanism for mRNA turnover is identical and whether it requires decapping of targeted transcripts by the Dcp1/Dcp2 complex or deadenylation by the Dhh1-interacting protein Pop2 (37). Moreover, it would also be interesting to elucidate which regions on Cth1 and Cth2 protein function as mRNA decay activation domains.

Some mRNA-specific regulatory proteins that recruit the translation repression and 5' to 3' decay machinery have been localized, at least transiently, to cytoplasmic P-bodies. In human cells, overexpressed TTP, as well as its targeted ARE-containing mRNAs, co-localize within P-bodies (20, 35). In yeast, the Rbp1 protein, which binds to the 3'-UTR of mitochondrial porin mRNA and promotes its degradation, has been localized to P-bodies under glucose starvation and hyperosmotic stresses and in *xrn1Δ* mutant cells (38). In this report we show that the Cth2 protein is trapped in the P-bodies of *dcp1Δ*, *dcp2Δ*, and *xrn1Δ* mutant cells (Fig. 5). This observation is consistent with a function of the decapping complex Dcp1/Dcp2 and the 5' to 3' exonuclease Xrn1 in the exit of Cth2 from P-bodies. We have also observed that the Cth2 protein does not accumulate in P-bodies in the absence of Lsm1 protein (Fig. 5), a component of the Lsm1-7 complex that functions in a rate-limiting step of decapping, and in wild type cells under stressful conditions including glucose starvation, osmotic stress, and stationary phase. These results suggest that the function of Cth2 may be the delivery of mRNAs to the decay site. Further experiments are required to ascertain whether the degradation of Cth2 target transcripts is necessary for Cth2 protein to leave the P-bodies and enter a new cycle of targeted mRNA degradation. Finally, Cth2 protein is not localized to P-bodies in other mRNA decay mutants assayed here, including *dhh1Δ*. This result was expected because these mutants do not accumulate P-bodies at early exponential phase, and in some cases, such as in *pat1Δ* and *dhh1Δ* mutants, a decrease in the assembly of P-bodies is observed as compared with wild type cells (16, 22).

Collectively, the data presented in this report strongly suggest that, in response to iron deficiency, the Cth2 protein promotes the 5' to 3' decay of *SDH4* mRNA by recruiting the Dhh1 helicase, a core component of P-bodies. Preliminary observations on the steady-state levels of other ARE-containing mRNAs regulated by Cth2, such as *ISA1*, indicate that its degradation is at least partially independent of Dhh1.<sup>7</sup> Furthermore, it has been recently proposed that the nuclear exonuclease Rat1 participates in the degradation of

*CTH2* mRNA, which contains a putative ARE sequence within its 3'-UTR (39). These observations suggest that, as previously shown for human TTP, Cth2 could promote the turnover of ARE-containing mRNA by multiple mechanisms. The challenge for future studies will be to understand how mRNA-specific regulators coordinate multiple mechanisms of post-transcriptional regulation.

*Acknowledgments*—We are grateful to the members of the Parker laboratory for helpful suggestions. We also thank Drs. Lola Peñarrubia and Caroline Decker for comments on the manuscript.

## REFERENCES

1. Baynes, R. D., and Bothwell, T. H. (1990) *Annu. Rev. Nutr.* **10**, 133–148
2. Kaplan, J., McVey Ward, D., Crisp, R. J., and Philpott, C. C. (2006) *Biochim. Biophys. Acta* **1763**, 646–651
3. Hentze, M. W., Muckenthaler, M. U., and Andrews, N. C. (2004) *Cell* **117**, 285–297
4. Masse, E., and Arguin, M. (2005) *Trends Biochem. Sci.* **30**, 462–468
5. Puig, S., Andres-Colas, N., Garcia-Molina, A., and Penarrubia, L. (2007) *Plant Cell Environ.* **30**, 271–290
6. Rouault, T. A. (2006) *Nat. Chem. Biol.* **2**, 406–414
7. Shakoury-Elizeh, M., Tiedeman, J., Rashford, J., Ferea, T., Demeter, J., Garcia, E., Rolfes, R., Brown, P. O., Botstein, D., and Philpott, C. C. (2004) *Mol. Biol. Cell* **15**, 1233–1243
8. Rutherford, J. C., Jaron, S., and Winge, D. R. (2003) *J. Biol. Chem.* **278**, 27636–27643
9. Courel, M., Lallet, S., Camadro, J. M., and Blaiseau, P. L. (2005) *Mol. Cell Biol.* **25**, 6760–6771
10. Puig, S., Askeland, E., and Thiele, D. J. (2005) *Cell* **120**, 99–110
11. Puig, S., Vergara, S. V., and Thiele, D. J. (2008) *Cell Metab.* **7**, 555–564
12. Parker, R., and Song, H. (2004) *Nat. Struct. Mol. Biol.* **11**, 121–127
13. Garneau, N. L., Wilusz, J., and Wilusz, C. J. (2007) *Nat. Rev. Mol. Cell Biol.* **8**, 113–126
14. Cheng, Z., Collier, J., Parker, R., and Song, H. (2005) *RNA* **11**, 1258–1270
15. Collier, J., and Parker, R. (2005) *Cell* **122**, 875–886
16. Sheth, U., and Parker, R. (2003) *Science* **300**, 805–808
17. Decker, C. J., Teixeira, D., and Parker, R. (2007) *J. Cell Biol.* **179**, 437–449
18. Parker, R., and Sheth, U. (2007) *Mol. Cell* **25**, 635–646
19. Eulalio, A., Behm-Ansmant, I., and Izaurralde, E. (2007) *Nat. Rev. Mol. Cell Biol.* **8**, 9–22
20. Kedersha, N., Stoecklin, G., Ayodele, M., Yacono, P., Lykke-Andersen, J., Fritzler, M. J., Scheuner, D., Kaufman, R. J., Golan, D. E., and Anderson, P. (2005) *J. Cell Biol.* **169**, 871–884
21. Teixeira, D., Sheth, U., Valencia-Sanchez, M. A., Brengues, M., and Parker, R. (2005) *RNA* **11**, 371–382
22. Teixeira, D., and Parker, R. (2007) *Mol. Biol. Cell* **18**, 2274–2287
23. Goldstrohm, A. C., Hook, B. A., Seay, D. J., and Wickens, M. (2006) *Nat. Struct. Mol. Biol.* **13**, 533–539
24. Blackshear, P. J. (2002) *Biochem. Soc. Trans.* **30**, 945–952
25. Lai, W. S., Carballo, E., Strum, J. R., Kennington, E. A., Phillips, R. S., and Blackshear, P. J. (1999) *Mol. Cell Biol.* **19**, 4311–4323
26. Lykke-Andersen, J., and Wagner, E. (2005) *Genes Dev.* **19**, 351–361
27. Fenger-Gron, M., Fillman, C., Norrild, B., and Lykke-Andersen, J. (2005) *Mol. Cell* **20**, 905–915
28. Chen, C. Y., Gherzi, R., Ong, S. E., Chan, E. L., Rajmakers, R., Puijng, G. J., Stoecklin, G., Moroni, C., Mann, M., and Karin, M. (2001) *Cell* **107**, 451–464
29. Hau, H. H., Walsh, R. J., Ogilvie, R. L., Williams, D. A., Reilly, C. S., and Bohjanen, P. R. (2007) *J. Cell. Biochem.* **100**, 1477–1492
30. Stoecklin, G., Mayo, T., and Anderson, P. (2006) *EMBO Rep.* **7**, 72–77
31. He, W., and Parker, R. (1999) *Methods* **17**, 3–10
32. Foury, F., and Talibi, D. (2001) *J. Biol. Chem.* **276**, 7762–7768

<sup>7</sup> E. Pedro-Segura and S. Puig, unpublished observations.

33. Thompson, M. J., Lai, W. S., Taylor, G. A., and Blackshear, P. J. (1996) *Gene (Amst.)* **174**, 225–233
34. Goldstrohm, A. C., Seay, D. J., Hook, B. A., and Wickens, M. (2007) *J. Biol. Chem.* **282**, 109–114
35. Franks, T. M., and Lykke-Andersen, J. (2007) *Genes Dev.* **21**, 719–735
36. Pilkington, G. R., and Parker, R. (2008) *Mol. Cell. Biol.* **28**, 1298–1312
37. Collier, J. M., Tucker, M., Sheth, U., Valencia-Sanchez, M. A., and Parker, R. (2001) *RNA* **7**, 1717–1727
38. Jang, L. T., Buu, L. M., and Lee, F. J. (2006) *J. Biol. Chem.* **281**, 29379–29390
39. Ciafis, D., Bohnsack, M. T., and Tollervey, D. (2008) *Nucleic Acids Res.* **36**, 3075–3084